James Webb Space Telescope optical simulation testbed IV: linear control alignment of the primary segmented mirror

Sylvain Egron[a,b,c], Rémi Soummer[a], Charles-Philippe Lajoie[a], Aurélie Bonnefois[b], Joseph Long[a], Vincent Michau[b], Elodie Choquet[d,e], Marc Ferrari[c], Lucie Leboulleux[a,b,c], Olivier Levecq[a], Johan Mazoyer[a], Mamadou N'Diaye[f], Marshal Perrin[a], Peter Petrone[a], Laurent Pueyo[a], and Anand Sivaramakrishnan[a]

[a]Space Telescope Science Institute, 3700 San Martin Drive, Baltimore, MD 21218, USA
[b]Office National d'Etudes et de Recherches Aérospatiales, 29 Avenue de la Division Leclerc, 92320 Châtillon, France
[c]Aix Marseille Université, CNRS, LAM (Laboratoire d'Astrophysique de Marseille) UMR 7326, 13388, Marseille, France
[d]Jet Propulsion Laboratory, California Institute of Technology, 4800 Oak Grove Drive, MS 169-506, Pasadena, CA 91109, USA
[e]Hubble Fellow
[f]Université Côte d'Azur, Observatoire de la Côte d'Azur, CNRS, Laboratoire Lagrange, Bd de l'Observatoire, CS 34229, 06304 Nice cedex 4, France

ABSTRACT

The James Webb Space Telescope (JWST) Optical Simulation Testbed (JOST) is a tabletop experiment designed to study wavefront sensing and control for a segmented space telescope, such as JWST. With the JWST Science & Operations Center co-located at STScI, JOST was developed to provide both a platform for staff training and to test alternate wavefront sensing and control strategies for independent validation or future improvements beyond the baseline operations. The design of JOST reproduces the physics of JWST's three-mirror anastigmat (TMA) using three custom aspheric lenses. It provides similar quality image as JWST (80% Strehl ratio) over a field equivalent to a NIRCam module, but at 633 nm. An Iris AO segmented mirror stands for the segmented primary mirror of JWST. Actuators allow us to control (1) the 18 segments of the segmented mirror in piston, tip, tilt and (2) the second lens, which stands for the secondary mirror, in tip, tilt and x, y, z positions. We present the most recent experimental results for the segmented mirror alignment. Our implementation of the Wavefront sensing (WFS) algorithms using phase diversity is tested on simulation and experimentally. The wavefront control (WFC) algorithms, which rely on a linear model for optical aberrations induced by misalignment of the secondary lens and the segmented mirror, are tested and validated both on simulations and experimentally. After alignment, JOST achieves 23 nm RMS WFE at 633 nm (RMS = lambda/28), which after accounting for the difference in design wavelengths, is comparable to the budgeted post-alignment WFE expected for JWST. We present the performance of the full active optic control loop in presence of perturbations on the segmented mirror, and we detail the quality of the alignment correction.

Keywords: JWST, Linear control alignment, Wavefront control, Wavefront Sensing

1. INTRODUCTION

The current generation of ground-based telescopes has large enough primary mirror diameters that active optical control based on wavefront sensing is necessary. Similarly, in space, while the Hubble Space Telescope (HST) has a mostly passive optical design, apart from focus control, its successor the James Webb Space Telescope (JWST) has active control of many degrees of freedom in its primary and secondary mirrors. JWST's wavefront

Further author information, send correspondence to Sylvain Egron: E-mail: sylvain.egron@lam.fr, Telephone: 1 410 338 6788

UV/Optical/IR Space Telescopes and Instruments: Innovative Technologies and Concepts VIII
edited by Howard A. MacEwen, James B. Breckinridge, Proc. of SPIE Vol. 10398, 1039811
 · doi: 10.1117/12.2272981

sensing and control (WFS&C) system will have to set the telescope into its alignment state after the deployment and maintain that alignment for the lifetime of the mission.[1] The wavefront sensing and control technologies chosen for the JWST have been substantially tested in simulation and experimentally. For that purpose, Ball Aerospace built a 1:6 scale mock up of JWST: The Testbed Telescope (TBT), which was used to achieve the necessary demonstrations of technology readiness in preparation for JWST.[2,3]

But WFS&C development remains an active field of research, with novel algorithms arising that may provide increased efficiency,[4] useful contingency capabilities for JWST,[5] or aid in its long term optical maintenance.[6] Developing the JWST Optical Simulation Testbed (JOST) at the Space Telescope Science Institute (STScI) provides a platform to test and evaluate new algorithms for WFS&C, with possible applications to JWST or to future missions such as the proposed Large UV/Optical/IR Surveyor (LUVOIR).[7] Moreover, this testbed will be helpful to develop staff expertise for JWST commissioning and operations reproducing various steps of the alignment. It is a supplement to existing verification and validation activities for independent cross-checks and novel experiments, not a part of the mission's critical path development process.
JOST is a simplified model of JWST, not an exact scaled model as in the case of the TBT. However it provides a close enough physical model so that the key optical aspects remain the same, especially for the degrees of freedom which are most relevant for maintenance over the life of JWST such as segment tilts and misalignment of the secondary relative to the primary. To meet that requirement, JOST is a three-lens anastigmat, a refractive analogue to JWST's three mirror anastigmat. A lens and aperture stop define JOST's entrance pupil, with segmentation provided by a segmented deformable mirror conjugated with that pupil (in the re-imaged pupil plane equivalent to where JWST's Fine Steering Mirror is located). JOST is designed to achieve similar quality image and image sampling as JWST at 2 microns ($>$ 80% Strehl ratio, and Nyquist sampled) over a field equivalent to the NIRCam module, but at 633 nm wavelength.

This paper presents the first experimental results of the WFS&C including the segmented mirror. Our group presented a general overview of JOST in Perrin et al.[8] (hereafter Paper I). Its detailed optical design and several trade studies were presented in Choquet et al.[9] (hereafter Paper II). The experimental implementation of the WFS&C on the testbed is described in Egron et al.[10] (hereafter Paper III). The experimental results regarding the linear control of L2 is described in ICSO 2016 proceeding Egron et al. (hereafter Paper IV). Now that the alignment of the three lenses has been validated, this paper is about the alignment of the segmented deformable mirror. We emphasize that one of the unique aspects of JOST is its ability to model arbitrary 5-degree-of-freedom misalignments of the primary, secondary, and tertiary lenses with respect to one another, which can result in field-dependent wavefront errors that may not be sensed on a single field point. In §2, we will focus on the testbed optical simulation and the pupil planes definition. In §3, we describe the implementation of wavefront sensing (WFS) and wavefront control (WFC) on JOST. In §4, we present the first results of the linear control of the segmented mirror, integrating WFS&C.

2. TESTBED DESCRIPTION

2.1 Optical simulation

The optical simulation of JOST is done with the Zemax OpticStudio 2017 software, and the overall infrastructure has been developed so that the experiment can be run either on the hardware or using Zemax as a realistic simulator. We can change the lenses and segment positions in Zemax using our python software (this is done with motors on the testbed, or directly on the IRIS-AO deformable mirror for the segments), and calculate a point spread function (PSF) instead of acquiring images with our CCD camera. Including all testbed optical components in the simulation gives us the possibility to analyze some vignetting effects, as well as projections effects on the DM. In order to have a reliable end-to-end alignment process through Zemax, it is critical that the Zemax simulation of JOST is as accurate as possible. Fig. 1 gives the layout and some details of the design.
In Zemax, the 18 different sub-apertures are described thanks to 18 configurations. In each of them, we define the position and shape of the segment. The geometry of the pupil mask is defined thanks to the "User Defined Aperture" feature of Zemax, and final images considering the 18 configurations at the same time are computed using the "Huygens PSF" feature of Zemax. Thanks to this set up, it is possible to apply perturbations on L2 and the segmented mirror, save PSF images as fits files, run the control loop, and correct for the alignment. This whole process is automated both on the experimental side and the simulation side.

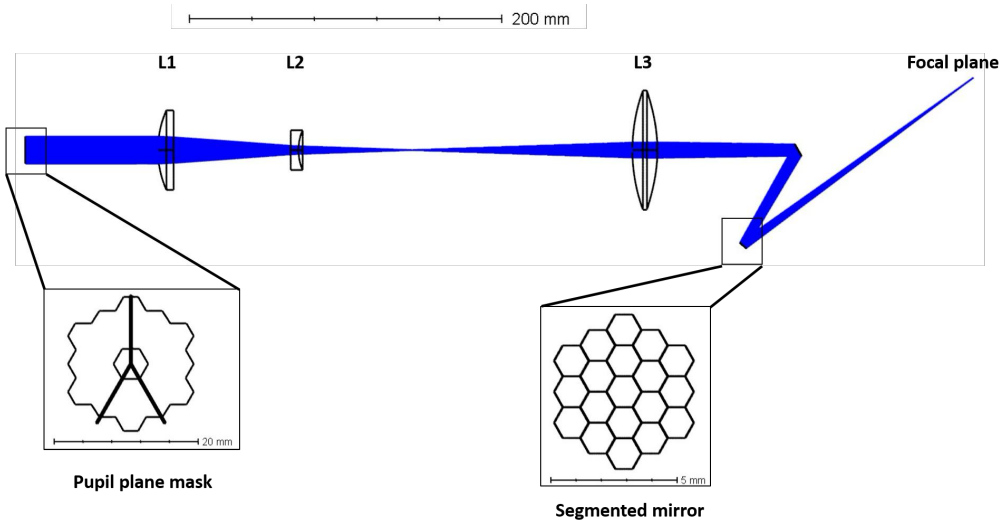

Figure 1. Optical layout for JOST. The pupil shape is defined by the pupil mask and the segmented mirror. The three lenses L1, L2 and L3 are the powered optics. In Zemax, the pupil plane mask is defined as a "user define aperture". The segmented mirror image gathers the 18 configurations of the Zemax file, each of which taking care of a different segment. Unlike in the actual JWST, the segments are not in the entrance pupil, but instead for practical reasons the segmented DM is located at the reimaged conjugate pupil after L3. This is analogous to the pupil plane where JWST's Fast Steering Mirror is located.

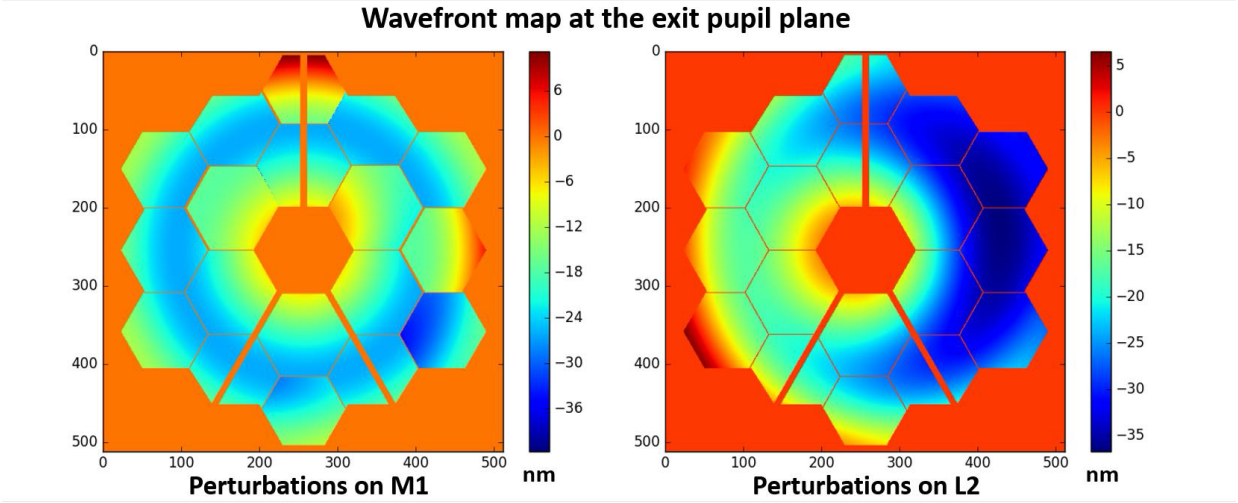

Figure 2. On the left: Wavefront maps with perturbations on the segments: 0.1 mm pistons on random segments and 0.05 degrees tip and tilts on other random segments. On the right: Wavefront maps with perturbations on L2: 0.1 mm decenter and 0.1 degrees tilt.

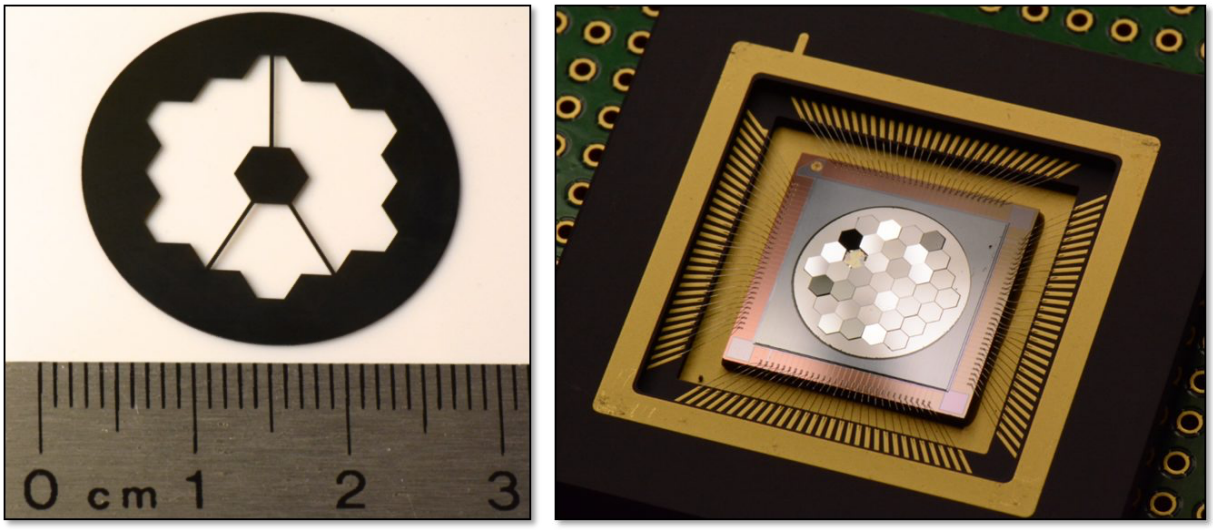

Figure 3. Photos of the optical elements defining the pupil plane on JOST. Left: JWST-like laser cut pupil mask. The secondary supports are 200 microns wide. Right: 37 segment Iris AO deformable mirror. This photo is of a spare Iris AO, which is not the device used on the testbed (missing segment). Each segment is only 1.4 mm in size; the entire 37-segment DM is less than 1 cm across. The inter-segment gaps are 10 microns wide. Note that we only use 18 of the 37 segments to create the JWST-like aperture. Together with the L1 lens these elements implement the surrogate segmented primary mirror for our testbed.

2.2 Pupil planes alignment

As a first step, the alignment of L1, L2, L3 was performed without the DM, over a full circular aperture (see paper IV). This section describes the new pupil shape and its components.

The JOST pupil is defined both by the entrance pupil mask and the segmented mirror. Photographs of pupil planes components are shown in Fig. 3. Both the deformable mirror (DM) and the pupil mask are conjugated to generate a pupil geometry similar to JWST with segments, including the 18 segments, the three spiders, the central obstruction, and the gaps between the segments. Lateral and clocking alignment were performed thanks to a pupil-imaging lens and our relocated camera to perform pupil imaging. Fig. 4 shows the experimental pupil image after pupil alignment.

3. COPHASING OF THE MIRROR

This section is dedicated to the alignment of the segmented mirror. We split it between the WFS and the WFC aspects.

3.1 Wavefront sensing

On JOST, WFS is achieved using linearized algorithm for phase diversity.[11] As shown in the previous section, we have a very good estimate of the pupil shape. In addition, a translation stage allows us to take two images - in focus and out of focus - of the PSF. These will be the inputs of the phase diversity algorithm.

In order to align the segmented mirror, we want to measure local piston, tip, tilt aberrations. Rather than considering the full aperture, the wavefront is described by the 18 different sub-apertures. In that configuration our output of the phase diversity is a vector of 18 by 3 sensing modes.

In reality, each JWST segment has more than 3 controllable degrees of freedom. However in practice they are sensed and controlled separately in different stages of commissioning. Sensing and controlling piston, tip, and tilt is consistent with the Fine Phasing stage of JWST commissioning and maintenance, which occurs after the other degrees of freedom are controlled in earlier steps of commissioning.

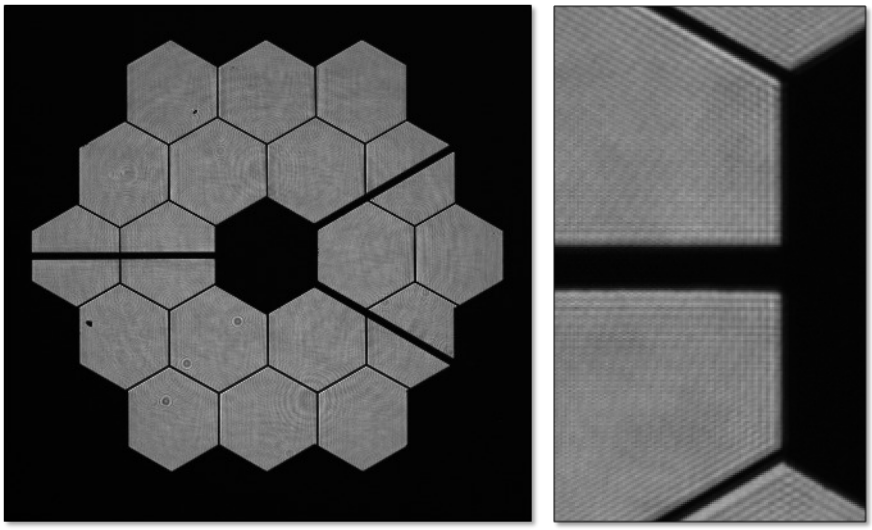

Figure 4. Experimental image of the pupil plane. On the left, image of the full pupil, on the right, a zoom close to the central obstruction. The pupil shape results in a combination of the pupil mask (spiders, central obstruction, global under size) and the segmented mirror (gaps between the segments).

3.2 Wavefront control

Wavefront control links the wavefront measurements to the mirror actuation. Projecting the wavefront onto the 18 sub-apertures is useful since the piston, tip, tilt aberrations measured are proportional to the piston tip, tilt position of the segment. 18 by 3 equations could be written to describe the wavefront from the segments positioning. Another way is to describe it using a matrix formalism:

$$\phi(\alpha) = J(\alpha) \times P, \tag{1}$$

where ϕ is the phase vector, P corresponds to the lens position vector, α is the field of observation and J is the Jacobian matrix.[12]

As a first approximation using a geometric approach, the perturbation applied to a segment will impact the wavefront only on the associated sub-aperture. Piston displacement will result as a local piston aberration (twice as big because of double pass). Tip and tilt angles on the segment will result as local tip, tilt aberrations (twice as large, because the reflected beam rotates twice as fast as the mirror does). It is easily predictable that the interaction matrix will be almost diagonal.[13] There are several reasons to explain why the matrix is not perfectly diagonal, and the the two principal ones are:

- Projection effects due to the DM tilt regarding the upcoming beam.
- The DM is in a converging beam rather than a collimated beam.

The least square approach of the problem consists in computing the generalized inverse of the matrix J. To do so, we use the singular value decomposition (SVD) of the Jacobian matrix (see papers III & IV).

4. EXPERIMENTAL RESULTS

4.1 Final alignment

The alignment of the segmented mirror was performed following the method described in the previous section. Fig. 5 illustrates our last results obtained on the testbed in May 2017. These ended the alignment process of the segmented mirror, and was compliant with the budget error of 40 nm wavefront error rms described in paper

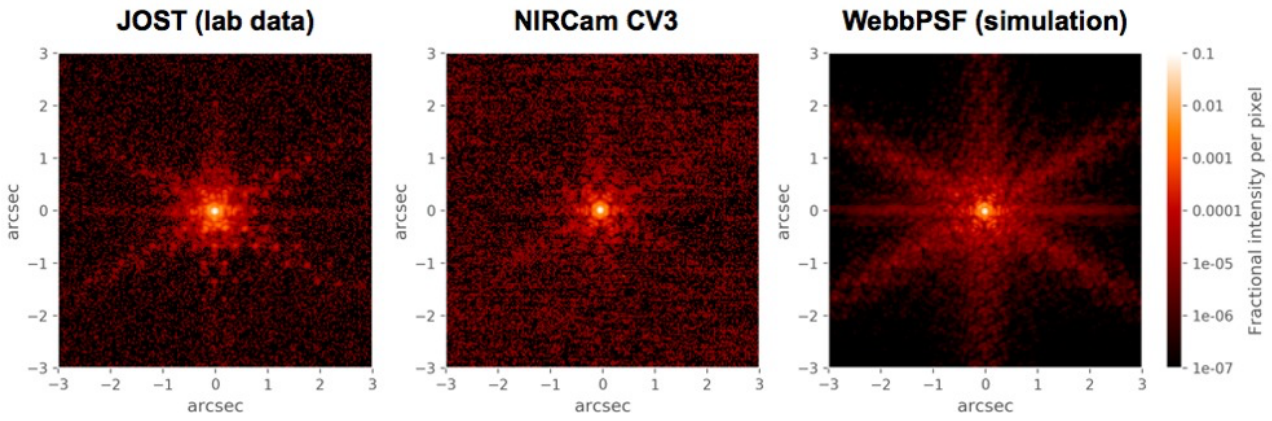

Figure 5. Experimental JOST data compared to NIRCam cryo-vacuum data in the F212N wavefront sensing filter, and simulated PSF with WebbPSF. The JOST data is 633 nm while the others are 2.12 microns. Also, the "angular scale in arcsec" on the JOST image is not the true angular scale on the testbed, but rather the equivalent scale that NIRCam would have for the same number of lambda/D. The experimental JOST PSF was obtained after close loop alignment of the DM. Piston, tip, and tilt of the segments were adjusted using linear control techniques. Even though the optical design and components of JOST are different from the ones of JWST, the proximity of these two PSF, confirms that the JOST design has the optical properties of JWST and can be considered as a hardware simulator of JWST.

II. This validates the alignment of both the lenses and the segmented mirror, as well as the wavefront sensing aspects.

In Figure 5 we compare the JOST experimental image with actual data taken with NIRCam during its ground testing (with a telescope simulator) and with a simulated image using WebbPSF.[8] This comparison confirms the optical proximity of JOST with JWST. The structure of the three PSF is very similar. The overall image quality (Strehl ratio), general PSF structure and sampling are extremely close for a hardware simulator. This fully validates JOST's goals to produce realistic-looking hardware-simulated JWST images. In particular, we note:

- The three main directions of the diffraction pattern due to the hexagonal shape of the segments.
- The horizontal diffraction line due to the vertical spider.
- High frequency features due to the gaps between the segments. Note that the ratio between the segment size and the gap size on the IRIS AO is similar to JWST's.

4.2 Alignment correction

Having the full testbed aligned allows us to implement and test correction loops. The current state of the testbed is what we consider to be the aligned state, or nominal state, since the remaining errors are not exceeding the requirements of the testbed.

Perturbations are now applied on the DM and the correction loop will aim at setting the testbed back to the nominal position. We have three ways to evaluate the correction success: tracking the alignment state at each iteration, looking at the shape of the final PSF, or looking at the phase map provided by the WFS part.

The next figures (Fig. 6&Fig. 7) show the performance of the control loop after applying perturbations to the segmented mirror: random piston, tip, and tilt perturbations, between -30 and +30 nm PtV, on all of the segments. The six images are the six PSFs (in log scale) obtained at the beginning of each iteration. First image is the one resulting from the applied aberration, before any correction. Through the iterations we recover the PSF theoretical shape of such an aperture. We can distinguish the first ring, and the three diffraction directions.

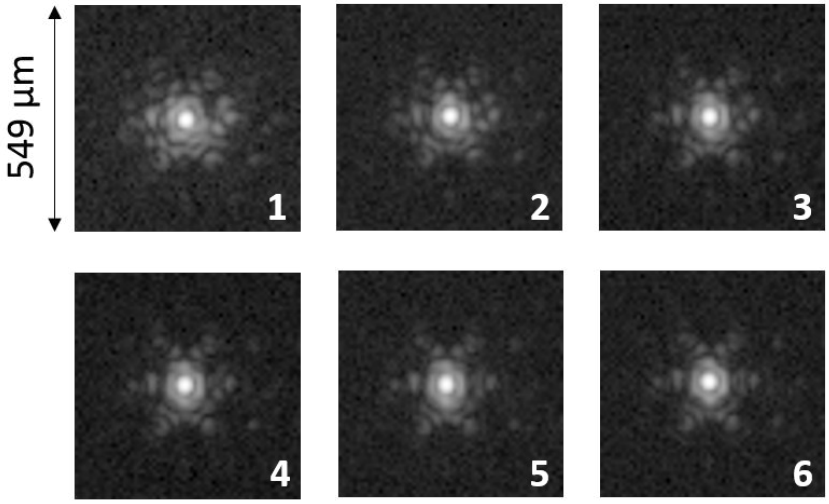

Figure 6. Experimental control loop result. From the top left to the bottom right, experimental JOST PSF, log scale, at each iteration of the control loop. Before image 1, a piston, tip and tilt perturbation has been applied on each of the 18 segments. The intensity of these local aberrations varying randomly between -30 and 30 nm PtV.

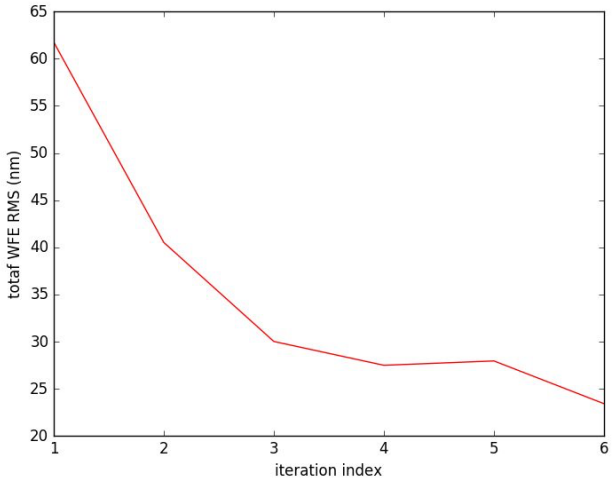

Figure 7. Experimental control loop result. Same experiment as the one described on Fig. 6. The plot gives the total WFE RMS (nm) at each iteration. The total WFE is dropping from 62 nm RMS (right after applying perturbations) to 23 nm RMS. After 6 iterations of the control loop, the JOST image quality requirements are fulfilled. These results experimentally validate the segmented mirror active control loop.

From the WFS point of view, Fig. 7 is a plot of the Wavefront error (WFE) RMS calculation in nm, at each iteration. Accordingly to the last image sequence, within 5 correction steps, the total WFE is dropping from 62 nm RMS to 23 nm RMS.

5. CONCLUSION

We have achieved the full automation of the JOST testbed, including control of the hardware, data acquisition, calibration, processing for wavefront sensing through focus-diverse phase retrieval, and wavefront control via a linear model. We use Python for high level scripting, and interface from Python to Zemax via Dynamic Data Exchange (DDE) for simulation.

The three lenses were initially aligned in x,y, and tip-tilt using an alignment telescope, and in z using a linear control model (described Paper IV). We have developed and experimentally validated the linear control infrastructure on the control of the segmented mirror. We are now ready for subsequent demonstrations of multi-field control with a segmented telescope. This is an unique aspect of JOST; many other lab wavefront control testbeds are optimized for a single field point (e.g. high contrast AO) or at most for multi-conjugate AO correction of a field about an arc minute across, and often just use DM surface figures to correct wavefront errors. JOST provides a test framework for optical alignment demonstrations for wide-field space telescopes, which requires active control of mirror positions and orientations in three dimensional space.

In the longer run, there may be more use of JOST to build further confidence in various contingency cases, alternate algorithms for example to improve operational efficiency. In any case, JOST will remain available as a training platform over years ahead as new staff members rotate onto the telescope team responsible for JWST's continued alignment. The state of the art in wavefront sensing techniques will surely continue to evolve during the perhaps decade-long lifetime of JWST. JOST's flexibility as a general purpose wavefront sensing testbed will allow it to address a wide range of questions or test relevant improved algorithms as needed. The testbed is also poised to evolve as a research platform to study segment phasing strategies for future space missions with larger numbers of segments. The development of such missions, such as the proposed LUVOIR, will be the work of many years.

ACKNOWLEDGMENTS

This work is supported by the JWST Telescope Scientist Investigation, NASA Grants NNX07AR82G and NNX15AC86G (PI: C. Matt Mountain).

EC acknowledges support from NASA through Hubble Fellowship grant HST-HF2-51355 awarded by STScI, operated by AURA, Inc. under contract NAS5-26555.

REFERENCES

[1] Acton, D. S., Knight, J. S., Contos, A., Grimaldi, S., Terry, J., Lightsey, P., Barto, A., League, B., Dean, B., Smith, J. S., Bowers, C., Aronstein, D., Feinberg, L., Hayden, W., Comeau, T., Soummer, R., Elliott, E., Perrin, M., and Starr, C. W., "Wavefront sensing and controls for the James Webb Space Telescope," Space Telescopes and Instrumentation **8442**, 84422H–84422H–11 (2012).

[2] Acton, D. S., Towell, T., Schwenker, J., Swensen, J., Shields, D., Sabatke, E., Klingemann, L., Contos, A. R., Bauer, B., Hansen, K., Atcheson, P. D., Redding, D., Shi, F., Basinger, S., Dean, B., and Burns, L., "Demonstration of the James Webb Space Telescope commissioning on the JWST testbed telescope," Proc. SPIE **6265** (July 2006).

[3] Acton, D. S., Towell, T., Schwenker, J., Shields, D., Sabatke, E., Contos, A. R., Hansen, K., Shi, F., Dean, B., and Smith, S., "End-to-end commissioning demonstration of the James Webb Space Telescope," Proc. SPIE **6687** (Sept. 2007).

[4] Jurling, A. S. and Fienup, J. R., "Extended capture range for focus-diverse phase retrieval in segmented aperture systems using geometrical optics," Journal of the Optical Society of America A **31**, 661 (Mar. 2014).

[5] Cheetham, A. C., Tuthill, P. G., Sivaramakrishnan, A., and Lloyd, J. P., "Fizeau interferometric cophasing of segmented mirrors," Optics Express **20**, 29457 (Dec. 2012).

[6] Greenbaum, A. Z., Gamper, N., and Sivaramakrishnan, A., "In Focus Phase Retrieval Using JWST-NIRISS' Non-Redundand Mask," Proc. SPIE **9904-159** (July 2016).

[7] Pope, B., Cvetojevic, N., Cheetham, A., Martinache, F., Norris, B., and Tuthill, P., "A demonstration of wavefront sensing and mirror phasing from the image domain," MNRAS **440**, 125–133 (May 2014).

[8] Perrin, M. D., Soummer, R., and Choquet, É., "James Webb Space Telescope Optical Simulation Testbed I: Overview and First Results," Proc. SPIE **9143**, 13 (2014).

[9] Choquet, É., Levecq, O., N'Diaye, M., Perrin, M. D., and Soummer, R., "James Webb Space Telescope Optical Simulation Testbed II: design of a three-lens anastigmat telescope simulator," Proc. SPIE **9143**, 91433T (2014).

[10] Egron, S., Lajoie, C.-P., Leboulleux, L., N'Diaye, M., Pueyo, L., Choquet, É., Perrin, M. D., Ygouf, M., Michau, V., Bonnefois, A., Fusco, T., Escolle, C., Ferrari, M., Hugot, E., and Soummer, R., "James Webb Space Telescope optical simulation testbed III: first experimental results with linear-control alignment," in [Space Telescopes and Instrumentation 2016: Optical, Infrared, and Millimeter Wave], **9904**, 99044A (July 2016).

[11] Mocœur, I., Mugnier, L. M., and Cassaing, F., "Analytical solution to the phase-diversity problem for real-time wavefront sensing," Optics Letters **34**, 3487 (Nov. 2009).

[12] Quirós-pacheco, F., Conan, J.-m., and Petit, C., "Generalized aliasing and its implications in modal gain optimization for multi-conjugate adaptive optics," Journal of the Optical Society of America A **27**(11), 182–200 (2010).

[13] Chapman, H. N. and Sweeney, D. W., "Rigorous method for compensation selection and alignment of microlithographic optical systems," Proc. SPIE **3331**, 102–113 (1998).